



	Experiment title: A pilot study to assess the possibilities of high resolution imaging of the mammal eye tissues	Experiment number: MD-1000
Beamline: ID17	Date of experiment: from: September 30 to: October 4, 2016	Date of report: Nov 29, 2016
Shifts: 12	Local contact(s): Alberto BRAVIN	<i>Received at ESRF:</i>

Names and affiliations of applicants (* indicates experimentalists):

Yury IVANISHKO^{2,3*}, Alberto BRAVIN^{1*}, Vladimir DMITRIEV¹, Sergey KOVALEV^{2,3*}, Polina LISUTINA^{2,3*}, Mikhail LOTOSHNIKOV^{2,3*}, Alberto MITTONE^{1*}, Sergey TKACHEV^{3*}, Marina TKACHEVA^{2,3}

¹European Synchrotron Radiation Facility, ID17, Grenoble, France

²Rostov Eye Clinic “InterYUNA”, Rostov-on-Don, Russia

³Rostov State Medical University, Central Scientific Research Laboratory, Rostov-on-Don, Russia

Report:

There are several complementary methods able to visualize the internal structures of eyes in clinics. Each clinical intravital imaging method is particularly suited in the diagnosis of pathologies affecting a specific zone of the eye. Despite the significant technological progress, the realization of images of the entire eyeball at the micrometric resolution is yet an unsolved task both in clinical diagnostics and in laboratory research. With this respect, high resolution images of the eyeball would be extremely useful, even in preclinical research, in the study of different pathologies of the retina, the lens, the optical nerve *etc.* In this work we combined the state of the art of micro computed tomography technology with phase contrast imaging, an innovative highly sensitive technique well adapted to investigate soft tissues without the use of contrast agents; we applied the technique in the post-mortem analysis of monkey eyes and rabbit eyes. A 3D visualization of the entire globe has been obtained for the first time with unprecedented resolution. These images show the potential of phase contrast imaging applied to the vision organ (*Fig. 1-2*). The success of this study open the way for *in vivo* imaging of the eye tissue with the highest levels of resolution and contrast, and the ability to visualize some of dynamic processes.

Methods:

The experiments were performed at the biomedical beamline (ID17) of ESRF. In order to apply the PBI technique, we used a quasi-monochromatic ($\Delta E/E \sim 10^{-4}$) quasi-parallel (divergence ≤ 1 mrad horizontally (H), and $\ll 0.1$ mrad, vertically (V)) X-ray beam. The monochromatic beam was selected from the continuous spectrum produced by the 21-pole wiggler source by a Si double Laue crystal monochromator system, installed at ID17, which is tuneable between 25 to 150 keV ($\lambda = 50-8$ pm). The maximum beam footprint on the sample was 150×7 mm² (HxV). The propagation distance between the sample and the detector was set to 11 meters. In order to perform the tomography scan the sample was rotated in front of the beam and images (projections) were acquired at different angles. The detection system was a sCMOS PCO edge 5.5 camera (2560x2160 pixels) connected with a 1:2X optics, holding a 350 μ m thick YAG-based scintillator screen to convert the X-rays into visible light. The imaging system pixel size was 3.2×3.2 μ m²; the detector Field of View (FoV) was about 8.2×7 mm² (HxV). Using the half-acquisition CT modality, the finally available FoV

was of about $16 \times 7 \text{ mm}^2$. Due to the limited available vertical field of view, which was smaller than the sample, the volumetric image of the eye was obtained by displacing it vertically twice in between two CT acquisitions.

The acquired images were reconstructed using the filtered-back projection algorithm after the application of the single defocused-image Paganin algorithm.

Samples:

Three kinds of samples were used in this experiment: **a)** formalin-fixed monkey eyes (*Macaca fascicularis*) enucleated post-mortem from adult specimens (embedded in an agar-agar preparation and included in transparent cylindrical plastic containers of 3 cm in diameter); **b)** enucleated eyes obtained post-mortem (immediately after enucleation were placed in a plastic cylinder containing a saline solution) from *Oryctolagus cuniculus* type HY107 rabbits and **c)** full heads from the same species (removed from the body post mortem, was fixed vertically in a specially designed holder, which allows to perform CT avoiding that the holder passes on FoV).

Dosimetry:

We measured the dose delivered in the different experimental conditions. The air kerma was measured using an ionization chamber, PTW Type 31002 Semiflex Tube Chamber 0.125 cm^3 calibrated at PTB and connected to the UNIDOS module. The dose distribution for head was then computed using Monte Carlo simulations. The model used in the simulations consisted in an elliptical shape of the dimensions of the rabbit head and the average dose was calculated in the region corresponding to the eye. The obtained values of doses vary according to the experimental parameters used during the acquisition within a range of [50,150] Gy. But preliminary results of time reduction down to few minutes for the image of the whole eyeball, and a consequent dose reduction down to ~ 2.5 Gy demonstrate that such reduction do not compromise the diagnostic significance of the images.

Results:

This study for the first time demonstrates the possibility of obtaining images of ocular structures using synchrotron radiation and phase-contrast imaging (Fig. 1-2). The discussed method allows visualizing soft tissue with the highest resolution and contrast, including a full 3D-model, without damaging the object under study and without requiring the use of contrast agents. The received results show the possibility of carrying out a similar study *in vivo* for intravital eye tissue imaging with previously unattainable resolution and the ability to visualize certain dynamic processes.

Acknowledgement:

We are grateful to ESRF for the beamtime and for the help provided to us by the local contacts and the ID17 team.

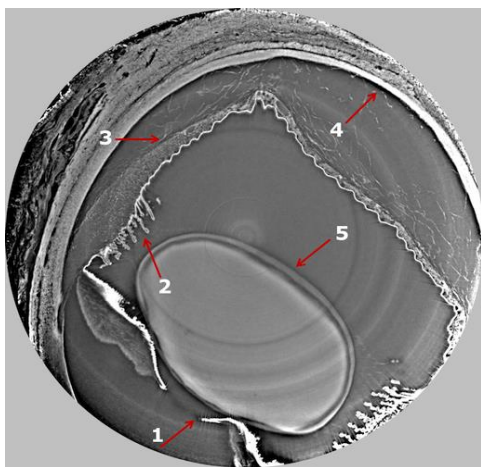


Figure 1: Cross-section of the monkey eye, centered on the lens. (1) the pupil and pupillary zone of the iris; (2) ciliary body; (3) detached retina; (4) sclera; (5) lens.

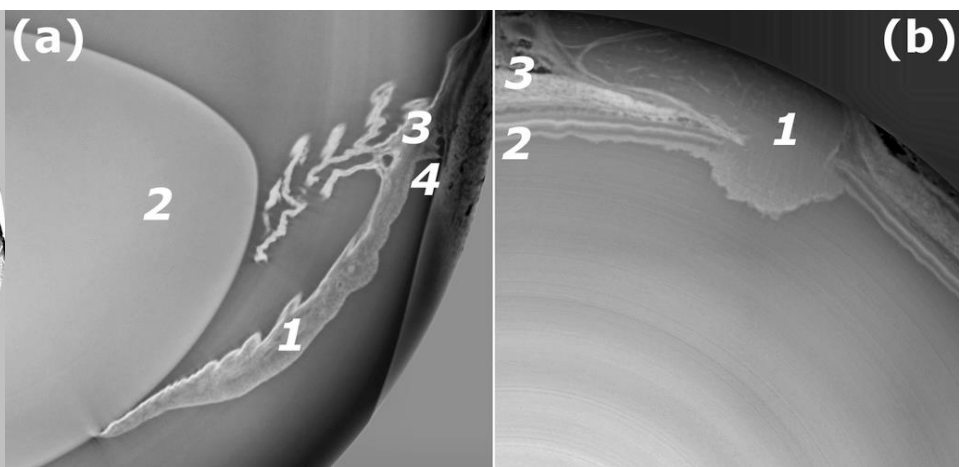


Figure 2: (a) iris (1), lens (2), ciliary body (3), anterior chamber angle (4) of isolated rabbit eye. (b) posterior pole of isolated rabbit eye — optical nerve (1), retina (2), sclera (3).